

# Cavity enhanced absorption and cavity enhanced magnetic rotation spectroscopy

Richard Engeln,<sup>a)</sup> Giel Berden, Rudy Peeters, and Gerard Meijer  
*Department of Molecular and Laser Physics, University of Nijmegen Toernooiveld,  
6525 ED Nijmegen, The Netherlands*

(Received 23 June 1998; accepted for publication 11 August 1998)

It is experimentally demonstrated that a narrow band continuous wave (cw) light source can be used in combination with a high-finesse optically stable cavity to perform sensitive, high-resolution direct absorption and optical rotation spectroscopy in an amazingly simple experimental setup, using ideas from the field of cavity ring down spectroscopy. Light from a scanning narrow band cw laser is coupled into the cavity via accidental coincidences of the laser frequency with the frequency of one of the multitude of modes of the cavity. The absorption and polarization rotation information is extracted from a measurement of the *time-integrated* light intensity leaking out of the cavity as a function of laser wavelength. © 1998 American Institute of Physics. [S0034-6748(98)01811-5]

## I. INTRODUCTION

In the field of cavity ring down (CRD) spectroscopy there is a trend to use narrow band continuous wave (cw) light sources<sup>1-4</sup> rather than pulsed light sources, for which the technique has originally been developed.<sup>5,6</sup> Not only is the data acquisition rate in a pulsed CRD experiment limited by the repetition frequency of the laser (typically 10–100 Hz), and is the spectral bandwidth in the best case Fourier transform limited (but typically  $0.1\text{ cm}^{-1}$ ), but the pulsed laser systems are also rather bulky and therefore less suited for, for instance, trace gas measurements outside of the laboratory. Although pulsed lasers do have the advantage that radiation can be produced over a wide wavelength range (in principle), it should be realized that the pulse energies delivered by commercially available laser systems are actually at the high end for what is required for CRD experiments. One could use less powerful, and preferably more compact (cheaper ?), light sources that are optimized for specific wavelength regions for these experiments as well. Ideally, the ever more readily available single-mode tunable diode lasers which can cover the visible and near-infrared spectral regions are used for these experiments.

When using narrow band cw lasers for CRD spectroscopy, one might at first think that thereby one of the biggest advantages and probably the main reason for the enormous success of CRD spectroscopy, i.e., the simplicity of the highly sensitive absorption detection setup, is thrown overboard, as now the cavity will have to be frequency locked to the laser (or *vice versa*). Although various schemes for locking of narrow band cw lasers to optical cavities have been successfully implemented in the past and although it is therefore well known how to proceed, the resulting experimental setup will certainly always be more involved than the “conventional” pulsed CRD setup.

Locking of the laser frequency to an external optical cavity is the only way to proceed when a large light intensity

in the “build-up” cavity is needed and when efficient use of the light source is required. This is for instance the case when background-free detection schemes [laser induced fluorescence (LIF), photoacoustic (PA) detection, bolometer detection, etc.] are used to monitor or detect, with the highest possible sensitivity, species present inside (or passing through) the cavity. The commonly used approach for this is to make a confocal cavity, i.e., to make the distance  $d$  between the mirrors that build up the optical cavity identical to the radius of curvature  $r$  of the two mirrors, and to actively adjust the length of the cavity such as to match the frequency of one of the longitudinal modes of the high finesse cavity to the laser frequency. When the optical cavity is merely used to perform efficient multipassing along a well-defined line, as in CRD absorption spectroscopy, the only requirement for the light intensity inside the cavity is that a sufficient amount of light leaks out of the cavity (per unit time) such that it can still be detected with a good signal-to-noise ratio, without being limited, for instance, by the noise of the detection system. In this case, one is allowed to use the accidental coincidences of the frequency of one of the modes in the optical cavity with the frequency of the laser to couple light into the cavity. Obviously, the efficiency of coupling light into the cavity is determined by the multitude of modes that can be excited in the cavity in combination with the frequency jitter of these modes relative to the laser frequency. A cavity with a quasicontinuum mode structure is obtained by choosing the mirror separation  $d$  within the stability regime, i.e.,  $0 < d < r$ ,  $r < d < 2r$ . It has been shown previously that an unstabilized cavity of this type enables semiefficient injection of (narrow band) light into the cavity.<sup>1,7</sup>

In this article we report on the use of narrow band cw light sources to perform cavity enhanced absorption (CEA) and cavity enhanced magnetic rotation (CEMR) spectroscopy. The radiation from a scanning narrow band cw laser is coupled into the cavity via the accidental coincidences of the laser frequency with the frequency of one of the multitude of modes of the cavity. The absorption and polarization rotation

<sup>a)</sup>Electronic mail: richarde@sci.kun.nl

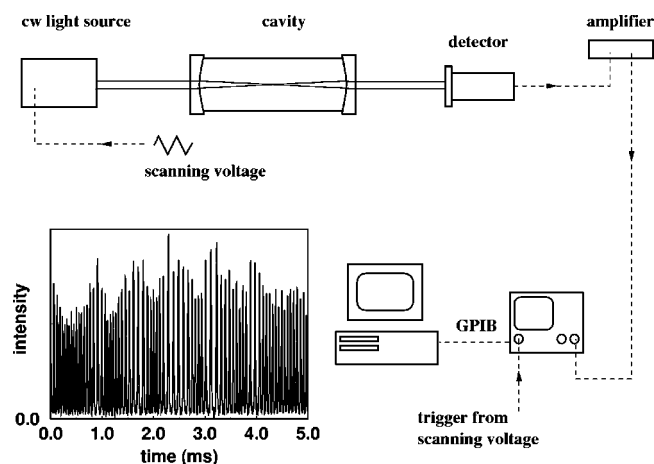


FIG. 1. Scheme of the experimental setup. Narrow band radiation from a rapidly scanning cw laser is coupled into an optical stable cavity when accidentally coincident with one of the cavity modes. The time-integrated intensity is detected and displayed on a digital oscilloscope. The inset shows a typical time-resolved intensity pattern as recorded at the exit of a 45-cm-long cavity, while scanning the laser over a  $0.115\text{ cm}^{-1}$  wide spectral region.

information is extracted from a measurement of the *time-integrated* light intensity that leaks out of the cavity. From a plot of the inverse of this intensity versus wavelength, the direct absorption and/or optical rotation spectra are obtained. Using diode lasers as well as a ring-dye laser, both the CEA and the CEMR technique are demonstrated by recording the appropriate spectra for oxygen, water, and ammonia in a cell, as well as by recording the spectra of molecular oxygen and ammonia in a slit-jet expansion.

## II. EXPERIMENTAL SETUP AND MEASUREMENT PROCEDURE

A scheme of the experimental setup is depicted in Fig. 1. As a light source we have used two single-frequency cw diode lasers (EOSI LCU 2010A and New Focus Model 6262) as well as an  $\text{Ar}^+$ -laser pumped single-frequency cw ring dye laser (Spectra Physics 380). The diode module in the EOSI laser covers the 750–780 nm region (up to 15 mW). The New Focus diode laser is tunable in the 1506–1595 nm region with 5 mW maximum power. The ring dye laser is operated on DCM to cover the spectral region of the  $\gamma$  band of molecular oxygen around 628 nm and delivers typically 200 mW. Both diode lasers have an external cavity and can be scanned mode-hop free by piezo tuning the end mirror. The ring dye laser is scanned mode-hop free by changing the cavity length with two galvo-driven plates. During all the experiments reported here the lasers are repeatedly scanned over a spectral range of typically  $1\text{ cm}^{-1}$  at a rate on the order of 5–100 Hz.

The narrow band cw laser radiation is coupled into a high finesse stable optical cavity, formed by two planoconcave mirrors with a diameter of 25 mm and a radius of curvature of  $-1\text{ m}$  and a specified optimum reflectivity of typically  $R=0.9999$ . In the cell experiments, the mirrors act as windows for the cell. When using short cells (5–20 cm), the mirrors are directly flanged onto a stainless steel tube and no further alignment of the mirrors relative to each other is

needed. Obviously, the cell as a whole is adjusted such as to couple in the laser-light efficiently. To avoid optical feedback from the cavity to the laser, the cell is positioned under a small angle with respect to the incoming laser beam or a Faraday isolator is used. When using longer cavities (25–90 cm), independent alignment of the two mirrors is required. The light that leaks out of the cavity is detected by either a photodiode or a photomultiplier tube (PMT). The detector signal is amplified and displayed on a digital oscilloscope. To record wavelength spectra, the oscilloscope is used in x-y mode, in which the horizontal axis is triggered by the voltage ramp used to scan the laser and is therefore proportional to the laser wavelength. In the inset of Fig. 1 the light intensity leaking out of a 45-cm-long empty cavity is shown as a function of the wavelength of the diode laser (around 765 nm; bandwidth several MHz). The horizontal axis corresponds to a total frequency range of  $0.115\text{ cm}^{-1}$ , which is about ten free spectral ranges (FSRs) of the optical cavity. During the wavelength scanning, which is linear in time, different transverse cavity modes are excited. As the (unstable) cavity will drift during scanning, the observed mode pattern is not expected to repeat perfectly. It is observed that light is coupled into the cavity at an approximate rate of  $10^4$  times per second. This rate strongly depends on the detailed mode structure of the cavity,<sup>7</sup> in combination with the scanning rate of the laser and the frequency jitter of the cavity modes, i.e., the “unstability” of the cavity.

If one were to make a single scan, and were to probe the absorption spectrum of species inside the cavity that way, it is evident from the inset, and it has been pointed out by others,<sup>8–10</sup> that spectral features that are narrower than the spacing between the modes (approximately 50 MHz in this particular example) would escape observation. In repeating this procedure over the same spectral region, and summing up the observed results, these “gaps” in the spectrum can be filled up, however, via “random interleaved sampling.” It should be noted at this point that each of the cavity modes is rather narrow (around 100 kHz in this case), and that the apparent width of the modes as observed in the inset is a mere reflection of the effective bandwidth of the laser during scanning, convoluted with the time response of the optical cavity and the time response of the detection system. The integrated intensity at each of the different modes depends linearly on the finite “resonance” time of, a fraction of, the spectral profile of the laser with the cavity mode. As in this particular example the resonance time is mainly determined by the scanning rate of the laser, which should therefore be identical for all the different cavity modes, the remaining observed intensity differences have to be attributed to different (diffraction) losses or in-coupling efficiencies for different transverse modes. This also explains the observed repetition of the intensity pattern, in which the FSR of the cavity can still be recognized.

In a “standard” cw CRD experiment, the absorption information is deduced from the time dependence of the intensity buildup and/or decay of an optical cavity when tuned into and/or away from resonance with the laser frequency. For this, a triggering system is required that actively controls when data taking has to start, together with fast detection

electronics.<sup>2-4</sup> From the observed time dependence the absolute value of the ‘‘ring-down’’ time  $\tau(\nu)$  is determined, which can be expressed as<sup>11,12</sup>

$$\tau(\nu) = \frac{d}{c(1-R+\kappa(\nu)d)}. \quad (1)$$

In an experiment, the total cavity loss  $1/c\tau(\nu)$  is plotted as a function of frequency, as this is directly proportional to the absorption coefficient  $\kappa(\nu)$ , apart from an offset which is mainly determined by the finite reflectivity of the mirrors. To record a complete spectrum, the laser is slowly scanned or stepped from one frequency to the other, much like in a pulsed CRD experiment.

In the cavity enhanced absorption method reported here, the laser is rapidly scanned in time and the signal on the detector is integrated over a time that, with a given scanning rate of the laser, is matched to the expected width of the spectral lines. Scanning the laser over  $1 \text{ cm}^{-1}$  at a 10 Hz repetition rate with an integration time of 1 ms, corresponds to a spectral integration over only  $0.01 \text{ cm}^{-1}$ . Several identical scans are summed on the oscilloscope to improve the measurement statistics. The data on the scope are transferred via general purpose interface bus (GPIB) to a PC for further analysis. When the inverse of the *time integrated* detector signal is plotted versus the wavelength of the laser (*vide infra*) absorption spectra over the full scanning range, spectra that are of comparable quality to those obtained via ‘‘conventional’’ pulsed or cw CRD spectroscopy, appear directly on the screen in a fraction of a second!

In choosing the optimum experimental parameters several considerations are important. The width of the individual cavity modes,  $\Delta\nu_{\text{cavity}}$ , is rather small (in the tens of kHz range) for the high-Q optical cavities used in these experiments, and is actually considerably smaller than the width of the spectral profile of the scanning laser. We assume in the following that the spectral profile of the laser is a block function with a width  $\Delta\nu_{\text{laser}} \gg \Delta\nu_{\text{cavity}}$  and is scanned linearly in time. When the laser is slowly scanned into resonance with a cavity mode, light intensity will gradually build up in the cavity. The exact time dependence of this process can be described using, for instance, the formalism as outlined by Zalicki and Zare in Appendix B of their article,<sup>8</sup> and depends on the details of the spectral profile of the laser, the properties of the optical cavity, and the scanning rate of the laser. The maximum intensity that can be reached inside the cavity is proportional to the spectral overlap of the laser profile with the profile of the cavity mode. As the spectral profile of the cavity mode is well approximated by a Lorentzian profile with a width proportional to the total cavity losses, i.e., proportional to  $1/\tau$ , and with an intensity proportional to  $\tau^2$ , the maximum intensity in the cavity is directly proportional to the ring-down time  $\tau$ . The light intensity inside the cavity will converge to this limiting value, provided that the laser stays in resonance with the cavity mode sufficiently long, i.e., provided that the scanning rate is small compared to the ratio of  $\Delta\nu_{\text{laser}}$  to  $\tau$ . When the laser is tuned out of resonance, the intensity in the cavity will exponentially decay in time, again governed by the time constant  $\tau$ .

In the upper part of Fig. 2 the calculated time depen-

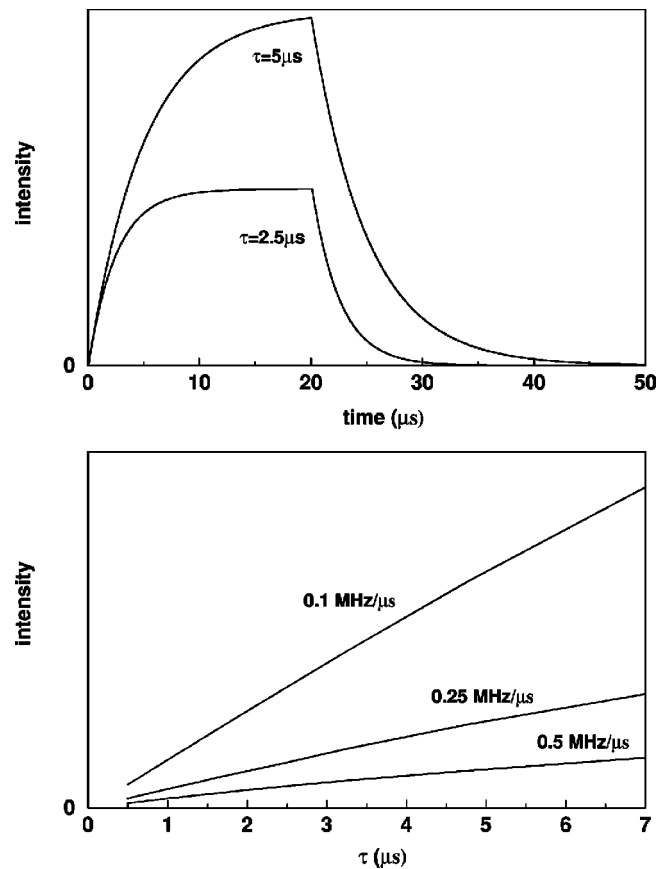


FIG. 2. Upper part: Calculated light intensity at the exit of a 15-cm-long optical cavity as a function of time. In the calculation, the spectral profile of the laser is assumed to be a block profile with a width of 5 MHz, scanned at a rate of 0.25 MHz/ $\mu\text{s}$ . Calculations are performed for round trip cavity losses of  $2 \times 10^{-4}$  ( $\tau = 5 \mu\text{s}$ ) as well as for losses that are twice as big. Lower part: Calculated integrated light intensity exiting the 15-cm-long cavity as a function of the photon lifetime  $\tau$  in the cavity, for three different values of the scanning rate of the laser.

dence of the light intensity behind a 15-cm-long cavity, having round trip losses of either  $2 \times 10^{-4}$  ( $\tau = 5 \mu\text{s}$ ) or  $4 \times 10^{-4}$  ( $\tau = 2.5 \mu\text{s}$ ), is shown. For these calculations a block profile with a width of 5 MHz and a scanning rate of 0.25 MHz/ $\mu\text{s}$  ( $\approx 8 \text{ cm}^{-1}/\text{s}$ ) is assumed for the laser. As the intensity decay when the laser is tuned out of resonance with the cavity mode follows a strict  $\exp(-t/\tau)$  time dependence, it is evident that the time-integrated signal behind the cavity would be exactly proportional to  $\tau$  if the intensity buildup would follow a  $[1 - \exp(-t/\tau)]$  dependence. Although the latter is not strictly true, it is explicitly shown in the lower part of Fig. 2 that the time-integrated intensity nevertheless follows a linear  $\tau$  dependence to a good approximation, and that this approximation gets better with lower scanning rates. Experimentally there is also a lower limit to the scanning rate, which is set by the requirement that all cavity modes should be in resonance with the laser more-or-less equally long, as otherwise large intensity fluctuations will occur. This implies that the scanning rate has to be significantly higher than the rate at which the cavity modes are jittering, or, alternatively, that one has to stabilize the cavity sufficiently to fulfill this requirement also for lower scanning rates. Even with the unstabilized optical cavities we used,

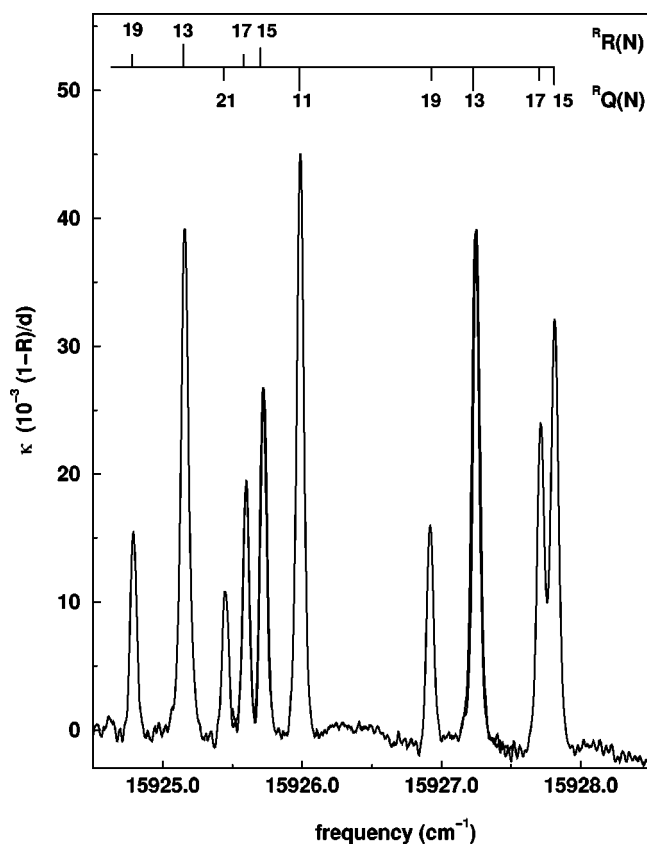


FIG. 3. Cavity enhanced absorption spectrum as recorded with 200 mbar molecular oxygen in a 12-cm-long cell at room temperature, displaying the bandheads in the  ${}^R R$  and  ${}^R Q$  branches of the  $b^1\Sigma_g^+(v'=2)\leftarrow X^3\Sigma_g^-(v''=0)$  transition.

there is a large “window” of scanning rates available in which both requirements are fulfilled. It is evident from the curves in the upper part of Fig. 2 that the light is actually coupled into the cavity as efficient as when the cavity is actively locked to the laser. This, combined with the strongly relaxed requirements on the light intensity behind the cavity as now the total time-integrated signal is used to extract the absorption information from, makes the power levels of commercially available diode lasers more than sufficient for these experiments.

### III. RESULTS AND DISCUSSION

In Fig. 3 a part of the absorption spectrum of the  $b^1\Sigma_g^+(v'=2)\leftarrow X^3\Sigma_g^-(v''=0)$  band of  ${}^{16}\text{O}_2$  ( $\gamma$  band), showing the bandheads of the  ${}^R R$  and  ${}^R Q$  branches, is shown as recorded with the cw ring dye laser in a 12-cm-long cell filled with 200 mbar of molecular oxygen at room temperature. The spectrum is a compilation of three partly overlapping measurements, each covering about  $1.5\text{ cm}^{-1}$  averaged over 100 scans. With a scanning rate of the laser of around 5 Hz, this implies an effective recording time of one minute. In the vertical direction, the inverse of the time-integrated intensity behind the cavity is plotted, with the baseline denoted as zero. The value of the baseline is proportional to  $(1-R)/d$ , but, contrary to CRD experiments, the absolute value of this quantity is not directly determined in this experiment. Therefore, the intensity scale of the spectrum is

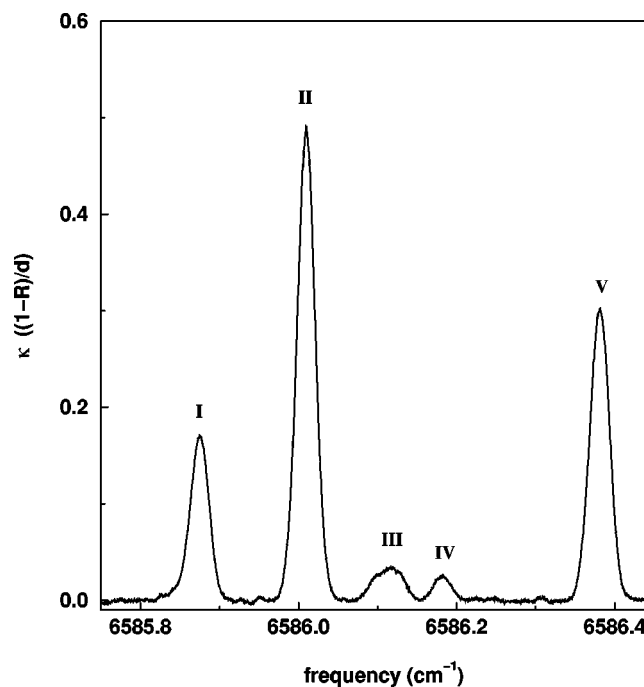


FIG. 4. Part of the CEA spectrum of a mixture of  $\text{H}_2\text{O}$  with a trace amount of  $\text{NH}_3$  at a total pressure of 1.0 mbar, measured in a 90-cm-long cell at room temperature. Transitions I and II originate from  $\text{H}_2\text{O}$  the others originate from  $\text{NH}_3$ .

expressed relative to the baseline intensity. This relative absorption spectrum can obviously be put on an absolute scale if the ring-down time of the empty cavity is known via some other way. If we do the reverse, and extract the effective mirror reflectivity  $R$  from the measured spectrum using the calculated population distribution of ground-state molecular oxygen and the known absorption cross sections for these transitions,<sup>13</sup> we deduce a reflection coefficient  $R=0.9998$ , in good agreement with independent CRD measurements.<sup>12</sup> The relative line intensities as observed in the spectrum match calculated absorption spectra very well, thereby explicitly demonstrating the viability of the data extraction procedure. It is worth noting that the noise level on the baseline of the spectrum is at the  $10^{-3}$  level, as good as can be obtained in standard CRD experiments. As mentioned in the previous section, the time axis of the digital oscilloscope which is used to average the traces is triggered by the ramp voltage used for scanning the laser. To accurately determine the absolute frequency position as well as to be able to correct for possible nonlinearities in the scanning, the well-known absorption spectrum of  $I_2$  is recorded simultaneously. The linewidth of the oxygen transitions is  $0.050\text{ cm}^{-1}$ , which is as expected from convoluting a Doppler broadened profile with a width of  $0.035\text{ cm}^{-1}$  with a pressure broadened profile with a width of, under our experimental conditions,  $0.024\text{ cm}^{-1}$ .<sup>14</sup>

One can of course always deduce absolute absorption coefficients from the CEA spectra, when the species whose absorption cross section or density is not known is measured simultaneously with a species with a known absorption coefficient. In Fig. 4 part of the CEA spectrum of a mixture of 1.0 mbar  $\text{H}_2\text{O}$  and a trace amount of  $\text{NH}_3$  is shown, as mea-

sured with the diode laser around 1518 nm in a 90-cm-long cell. Due to the lower reflectivity of the mirrors used in this setup ( $R \approx 0.9992$ ), the laser could be scanned over the approximate  $0.7 \text{ cm}^{-1}$  region at a rate of 100 Hz. The light that leaks out of the cavity is detected by a InGaAs photodiode detector and amplified with a 0.1 ms rise time amplifier. The spectrum shown is the average over 1000 consecutive scans and is acquired in 10 s. The  $\text{H}_2\text{O}$  transitions are the  $6_{51} \leftarrow 5_{42}$  (I) and the  $6_{52} \leftarrow 5_{41}$  (II) rotational transitions of the  $(1,1,3) \leftarrow (0,0,0)$  vibrational band, and have integrated absorption cross sections of  $1.13 \times 10^{-24}$  and  $3.39 \times 10^{-24} \text{ cm}^{-1} \text{ cm}^2/\text{mole}$ , respectively.<sup>15</sup> Peaks III to V in the spectrum are all due to  $\text{NH}_3$  but are as yet unassigned. The absorption cross section of peak V has been reported, however, as  $1.21 \times 10^{-21} \text{ cm}^{-1} \text{ cm}^2 \text{ mole}^{-1}$ ,<sup>16</sup> and a partial pressure of ammonia in our cell of  $1.7 \times 10^{-3}$  mbar is thus deduced. There are other  $\text{NH}_3$  lines in the tuning range of this diode laser with an order of magnitude larger cross section. In view of the signal-to-noise ratio of the current spectrum, partial pressures of  $10^{-6}$  mbar of ammonia will be detectable in this setup on these more favorable transitions.

The applicability of the CEA detection technique to molecular jets, is demonstrated here by presenting absorption spectra of individual rotational lines of the  $b^1\Sigma_g^+(v'=0) \leftarrow X^3\Sigma_g^-(v''=0)$  band of expansion cooled molecular oxygen, using a diode laser around 762 nm. A detailed spectroscopic study on jet-cooled ammonia, of which CEA spectra have been recorded in the  $1.5 \mu\text{m}$  region, will be reported elsewhere. A planar jet is formed by expanding a gas mixture of 30%  $^{16}\text{O}_2$  in Ar through a  $40 \text{ mm} \times 0.03 \text{ mm}$  slit nozzle. At a stagnation pressure of 760 Torr a  $1200 \text{ m}^3/\text{h}$  roots pump (Edwards EH1200) backed by a  $180 \text{ m}^3/\text{h}$  rotary pump (Leybold SV180) reaches a background pressure of 0.5 Torr.<sup>17</sup> The mirrors that form the optical cavity are now positioned 10 cm apart, with the cavity axis being along the long axis of the slit nozzle, intersecting the jet within a few mm from the orifice. In Fig. 5 the CEA spectrum of the  $^P P_1(1)$  transition of molecular oxygen as measured in this planar jet is shown. The spectrum is recorded by averaging over 500 scans with the laser scanning the  $0.25 \text{ cm}^{-1}$  spectral region at a 15 Hz rate, i.e., the spectrum is recorded in approximately 30 s. A narrow line with a full width at half maximum of 270 MHz is seen on top of a broad background. The background signal is mainly attributed to thermalized oxygen gas in the optical cavity outside of the expansion region. Contrary to CRD absorption spectroscopy, the CEA method is sensitive to the intensity profile of the diode laser over the spectral region that is scanned, which in the present case gives an additional minor contribution to the structured background signal. The observed linewidth is in accordance with the width of 80 MHz that is observed in direct absorption measurements on  $\text{C}_2\text{H}_4$  in a similar planar jet at roughly a factor of four longer wavelengths.<sup>17</sup> The observed line width of 270 MHz is less than 20% of the FSR of the optical cavity that is used, and the spectrum therefore exemplifies that the random interleaved sampling due to the frequency jitter of the unstabilized, multimode, cavity can be rather efficient indeed.

The CEA detection technique reported here, can be used to measure optical rotation spectra, when a polarization ana-

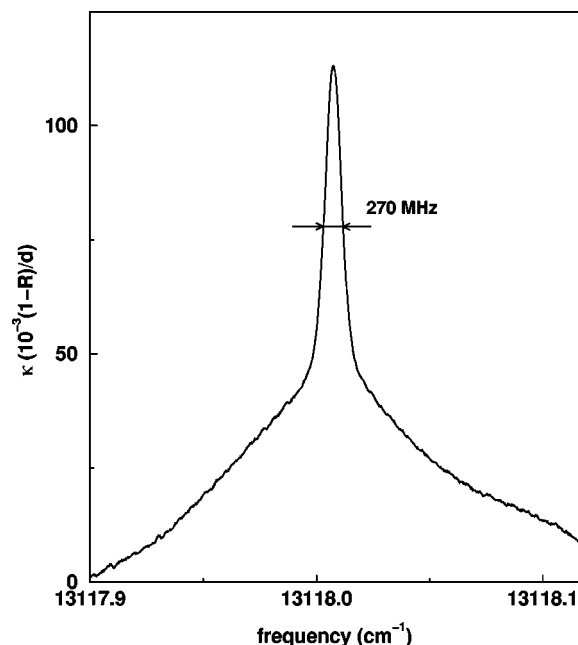


FIG. 5. CEA spectrum of the  $^P P_1(1)$  transition of the  $b^1\Sigma_g^+(v'=0) \leftarrow X^3\Sigma_g^-(v''=0)$  band of  $^{16}\text{O}_2$  measured in a 10-cm-long optical cavity positioned around a slit-jet expansion. The observed line width of 270 MHz is due to residual Doppler broadening in the jet, and is less than 20% of the FSR of the optical cavity.

lyzer is placed in front of the detector. We have recently theoretically outlined and experimentally demonstrated that polarization spectroscopy can be combined with pulsed CRD spectroscopy. In particular, we demonstrated that the optical rotation of molecular oxygen placed in a magnetic field can be sensitively and quantitatively determined in such a pulsed polarization dependent CRD detection scheme.<sup>12</sup> Using this same model system, i.e., the  $^P P_1(1)$  transition of the  $\gamma$  band of molecular oxygen in a magnetic field, we here demonstrate that sensitive cavity enhanced magnetic rotation spectroscopy can be performed as well. The experimental CEMR setup is only slightly different from the CEA setup described earlier. Prior to entering the optical cavity the laser beam passes through a Glan-Thompson polarizer with an extinction of  $10^{-5}$  to better define the polarization state of the incoming light. The 12-cm-long optical cavity is filled with 200 mbar of oxygen and placed inside a magnet which produces a homogeneous magnetic field up to 0.88 T over the whole length of the cell, perpendicular to the axis of the optical cavity (Voigt configuration). The polarization of the light that enters the cavity makes an angle  $\phi_B = 45^\circ$  relative to the direction of the magnetic field  $\mathbf{B}$ . A second Glan-Thompson polarizer is placed between the end mirror of the cell and the detector. The polarization direction of the light that is transmitted by this analyzer makes an angle  $\phi_D$ , relative to the polarization direction of the incoming light, and can be set with an accuracy of  $0.1^\circ$ .

In Fig. 6 the inverse of the time-integrated light intensity passing through the analyzer is shown as a function of frequency in the spectral region of the  $^P P_1(1)$  transition of the  $b^1\Sigma_g^+(v'=2) \leftarrow X^3\Sigma_g^-(v''=0)$  band of molecular oxygen for seven different values of the angle  $\phi_D$ . Each spectrum is an average over 100 scans, measured with a 5 Hz repetition

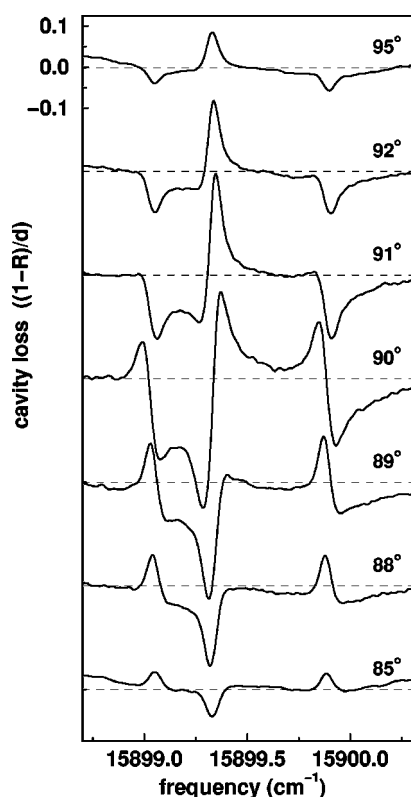


FIG. 6. Cavity enhanced magnetic rotation spectra of the  $^P P_1(1)$  transition of the  $b^1 \Sigma_g^+(v'=2) \leftarrow X^3 \Sigma_g^-(v''=0)$  band of molecular oxygen as recorded in a magnetic field of 0.88 T (Voigt configuration) using a 12-cm-long optical cavity filled with 200 mbar oxygen, measured as function of the angle  $\phi_D$ .

rate, and takes thus only 20 s to record. The vertical scale is the same for all seven spectra, and is only indicated as such for the uppermost spectrum, again in units relative to the baseline intensity. We demonstrated in our previous study that for detection angles  $\phi_D$  sufficiently far away from the crossed geometry, exponentially decaying transients result which are exclusively sensitive to polarization dependent absorptions (magnetic dichroism).<sup>12</sup> Both the upper two and the lower two spectra shown in Fig. 6 meet this requirement reasonably well. To interpret these spectra, we can therefore directly adapt Eq. (6) of Ref. 12 to our present situation, as the time-integrated intensity will again be proportional to the ring-down time for the specific analyzer direction  $\phi_D$  in this case. We thus find that the inverse of the time-integrated intensity is given by a term that is approximately proportional to  $[\kappa_{\parallel}(\nu) - \kappa_{\perp}(\nu)]/\cos(\phi_D)$  on top of a baseline, in which  $\kappa_{\parallel}(\nu)$  and  $\kappa_{\perp}(\nu)$  correspond to the absorptions polarized parallel ( $\Delta M = \pm 1$ ; outer two peaks) and perpendicular ( $\Delta M = 0$ ; central peak) to the magnetic field, respectively.<sup>12</sup> This equation explains the observed sign difference between the two types of transitions, the intensity increase upon approaching  $\phi_D = 90^\circ$  as well the overall sign change upon passage through the crossed polarizer geometry.

The central spectrum in Fig. 6, recorded with the crossed polarizer geometry, exclusively shows the effect of optical rotation due to dispersion. If the polarizers are indeed exactly crossed, it is obvious that any polarization rotation is expected to lead to an increase in the time-integrated intensity

behind the cavity, contrary to the observation where both increasing and decreasing signals are observed. The observations can therefore only be explained when a slight polarization rotation induced by the mirrors is taken into account as well. If we assume that, apart from the contribution of the magnetic circular birefringence of molecular oxygen, the mirrors introduce a small phase shift between the two mutually orthogonal polarization directions, the observed spectrum can be well understood. The remaining two spectra, recorded  $1^\circ$  away from the crossed polarizer configuration, contain all the possible contributions to polarization rotation that have been mentioned up to now, and are a weighed sum of the spectra that have been discussed.

We have demonstrated a simple yet sensitive experimental scheme to record high-resolution optical absorption and/or optical rotation spectra of molecules in open air, cells or jets, using ideas from the field of CRD spectroscopy. Light from a narrow band cw laser is coupled into a high-finesse stable optical cavity when accidentally coincident with one of the multitude of modes of this cavity. While rapidly scanning the narrow band laser, the time-integrated intensity exiting the cavity is monitored. Under the conditions that the scanning laser is sufficiently long in resonance with one of the cavity modes that the light intensity inside the cavity approaches its limiting value, the time-integrated light intensity exiting the cavity is in a good approximation proportional to the ring-down time  $\tau$ . Direct absorption spectra and/or optical rotation spectra can therefore be obtained by plotting the inverse of the time-integrated intensity versus the laser frequency. With a single mode laser scanning over typically a  $1 \text{ cm}^{-1}$  spectral region scanning rates of 5–100 Hz have been employed in this study, yielding high quality spectra in a matter of seconds. The noise equivalent detection limit readily approaches  $10^{-3}$  of the baseline intensity, fully comparable to the best CRD spectra reported to date. As the spectral information is deduced from the time-integrated signal rather than from the time dependence of the signal it is possible to perform these measurements with relatively low power lasers and cheap detection systems.

*Note added in proof.* A fully equivalent experimental approach is to scan the laser slowly and to rapidly scan the length of the cavity, linearly and repeatedly, by mounting one cavity mirror on a piezo electric crystal. The same conditions as mentioned in the paper, i.e., that the laser frequency is sufficiently long in resonance with one of the cavity modes that the light intensity inside the cavity approaches its limiting value, has to be fulfilled. Although this method is experimentally slightly more involved, it circumvents possible problems associated with averaging nonperfectly matched frequency scans. Since the submission of this paper we have experimentally verified that the latter approach can be used as well.

Obviously, measurement of the time-integrated light intensity behind the cavity can also be used in a pulsed CRD experiment to determine  $\tau$ ,<sup>18</sup> since  $\int_0^\infty I_0 \exp(-t/\tau) dt = I_0 \tau$ . However, the large pulse-to-pulse fluctuations in the intensity behind the cavity ( $I_0$ ) will limit the SNR ratio that can be obtained. In the recently reported “(time-) integrated cavity output analysis” scheme<sup>18</sup> normalization is accomplished

by measuring  $I_0$  in a time-resolved measurement, making this scheme identical to existing schemes in which the cavity decay time is determined using a two-channel boxcar averager.<sup>19</sup>

## ACKNOWLEDGMENTS

This work is part of the research program of the “Stichting voor Fundamenteel Onderzoek der Materie (FOM),” which is financially supported by the “Nederlandse Organisatie voor Wetenschappelijk Onderzoek (NWO).” The work is supported in part by the National Institute of Public Health and the Environment (RIVM). We acknowledge Dr. J. Oomens for making the slit-expansion setup available to us for these experiments.

<sup>1</sup>R. Engeln, G. von Helden, G. Berden, and G. Meijer, *Chem. Phys. Lett.* **105**, 262 (1996).

<sup>2</sup>D. Romanini, A. A. Kachanov, N. Sadeghi, and F. Stoeckel, *Chem. Phys. Lett.* **264**, 316 (1997).

<sup>3</sup>B. A. Paldus, J. S. Harris, J. Martin, J. Xie, and R. N. Zare, *J. Appl. Phys.* **82**, 3199 (1997).

<sup>4</sup>Y. He, M. Hippler, and M. Quack, *Chem. Phys. Lett.* **289**, 527 (1998).

<sup>5</sup>A. O’Keefe and D. A. G. Deacon, *Rev. Sci. Instrum.* **59**, 2544 (1988); A.

O’Keefe, J. J. Scherer, A. L. Cooksy, R. Sheeks, J. Heath, and R. J. Saykally, *Chem. Phys. Lett.* **172**, 214 (1990).

<sup>6</sup>M. D. Wheeler, S. M. Newman, A. J. Orr-Ewing, and M. N. R. Ashfold, *J. Chem. Soc., Faraday Trans.* **94**, 337 (1998), and references therein.

<sup>7</sup>G. Meijer, M. G. H. Boogaarts, R. T. Jongma, D. H. Parker, and A. M. Wodtke, *Chem. Phys. Lett.* **217**, 112 (1994).

<sup>8</sup>P. Zalicki and R. N. Zare, *J. Chem. Phys.* **102**, 2708 (1995).

<sup>9</sup>J. T. Hodges, J. P. Looney, and R. D. van Zee, *J. Chem. Phys.* **105**, 10 278 (1996).

<sup>10</sup>K. K. Lehmann and D. Romanini, *J. Chem. Phys.* **105**, 10 263 (1996).

<sup>11</sup>R. T. Jongma, M. G. H. Boogaarts, I. Holleman, and G. Meijer, *Rev. Sci. Instrum.* **66**, 2821 (1995).

<sup>12</sup>R. Engeln, G. Berden, E. van den Berg, and G. Meijer, *J. Chem. Phys.* **107**, 4458 (1997).

<sup>13</sup>The absolute intensities of the rotational lines in Fig. 3 can be calculated using the absorption cross section of the  $P(1)$  transition determined by CRD spectroscopy [from Fig. 3(a) of Ref. 12] and the relative intensities from a calculation of the rotational line strengths (Ref. 14).

<sup>14</sup>K. J. Ritter and T. D. Wilkerson, *J. Mol. Spectrosc.* **121**, 1 (1987).

<sup>15</sup>HITRAN (acronym for high resolution transmission molecular absorption) database (<http://www.hitran.com>).

<sup>16</sup>L. Lundsberg-Nielsen, F. Hegelund, and F. M. Nicolaisen, *J. Mol. Spectrosc.* **162**, 230 (1993).

<sup>17</sup>J. Oomens, L. Oudejans, J. Reuss, and A. Fayt, *Chem. Phys.* **187**, 57 (1994).

<sup>18</sup>A. O’Keefe, *Chem. Phys. Lett.* **293**, 331 (1998).

<sup>19</sup>D. Romanini and K. K. Lehmann, *J. Chem. Phys.* **99**, 6287 (1993).